

## Depth Profiling of Chemical and Electronic Structures and Defects of Ultrathin HfSiON on Si(100)

S. Miyazaki<sup>a</sup>, A. Ohta<sup>a</sup>, S. Inumiya<sup>b</sup>, Y. Nara<sup>b</sup> and K. Yamada<sup>c</sup>

<sup>a</sup>Graduate School of Advanced Sciences of Matter, Hiroshima University  
1-3-1 Kagamiyama, Higashi-Hiroshima 739-8530, Japan

<sup>b</sup>Semiconductor Leading Edge Technologies Inc.  
16-1 Onogawa, Tukuba 305-8501, Japan

<sup>c</sup>Nanotechnology Research Laboratories, Waseda University  
Shinjuku, Tokyo 162-0041, Japan

We present in-depth profiling of chemical bonding features and defect state density in ultrathin HfSiO<sub>x</sub>N<sub>y</sub> (Hf/(Hf+Si)≈43%) films with average nitrogen contents up to ~18at.% by using x-ray photoelectron spectroscopy (XPS) and total photoelectron yield spectroscopy (PYS) in combination with oxide thinning in a dilute HF solution. The films were prepared on pre-cleaned Si(100) by an atomic layer chemical vapor deposition (ALCVD) method and followed by plasma nitridation. By annealing at 1050°C in N<sub>2</sub> ambience, Si-N bonding units in the films are increased as a result of thermal decomposition of Hf-N<sub>x</sub> (x=2 and 3) units and the interfacial oxidation accompanied with nitrogen incorporation is caused. For the annealed samples, Hf ions coordinated with two N atoms are distributed with a profile peaked around 1nm from the top surface. Also, from the depth profiles of chemical compositions, which were determined from the change in the intensity at each thinning step, we found that the oxygen content becomes its minimum around ~1.2nm from the surface while the nitrogen content becomes its maximum within ~1.5nm from the surface. The result suggests that the surface re-oxidation is promoted coincidentally with the diffusion of N atoms generated by thermal decomposition of the Hf-N<sub>x</sub> units during the N<sub>2</sub>-annealing. The photoelectron yield from filled defect states in the dielectric stacks was increased in the early stages of oxide thinning and then decreased with further progressive thinning. The depth profile of the defect states, which was derived from the change in the yield, shows that the defect state density becomes its maximum in the near-surface region where oxygen deficiency becomes significant. It is likely that the imbalance in chemical coordination between anions and cations is responsible for the defect generation.

### Introduction

Continuous scaling of complementary metal-oxide-semiconductor (CMOS) devices to sub-50nm technology nodes has required urgently the replacement of a conventional gate dielectric stack with a physically-thicker high-k gate dielectric stack in order to suppress gate leakage below some allowable limits and to achieve higher capacitive coupling between the gate and the channel with an electrically-thinner equivalent SiO<sub>2</sub> thickness (1). However, there remain formidable technological challenges regarding the

control of interfacial reactions and electrically active defects in high-k gate stacks to settle degradations in channel mobility and threshold voltage controllability, and issues on dielectric reliability (2).

Among other high-k dielectrics, hafnium-based oxides such as Hf-silicates and Hf-aluminates have been intensively studied as most promising alternative gate dielectrics (3, 4) because of their moderate dielectric constants, favorable band alignments to Si(100) showing high potential barrier heights and relatively good thermal stability. Nitrogen incorporation into Hf-silicates has received much attention because it enables us to secure excellent thermal stability against crystallization and phase separation in annealing up to  $\sim 1100^{\circ}\text{C}$  and to improve diffusion barrier properties against impurity and oxygen atoms (5, 6), and practical advantages in increasing dielectric constant with nitrogen content (6) and improving overall reliability with optimizing nitrogen incorporation (7) have been reported so far. However, because there are some drawbacks that gate leakage current and/or fixed charge density increase with nitrogen incorporation, the control of nitrogen incorporation in Hf-silicates is a key for good FET performance with keeping a low leakage current. Thus, for a guideline how to optimize the nitrogen incorporation, the correlation between chemical structures and defect states in the  $\text{HfSiO}_x\text{N}_y$  has yet to be studied in detail.

In this work, we focused on depth profiling of chemical composition, bonding features and defect states in ultrathin  $\text{HfSiO}_x\text{N}_y$  layers formed on Si(100) with different nitrogen contents by using high-resolution x-ray photoelectron spectroscopy (XPS) and total photoelectron yield spectroscopy (PYS).

## Experimental

$\sim 5\text{-nm}$ -thick  $\text{HfSiO}_x$  films with a Hf content of  $\sim 43\%$  in  $\text{Hf}/(\text{Hf}+\text{Si})$  were deposited on pre-cleaned p-Si(100) wafers 300mm in diameter by an atomic layer chemical vapor deposition (ALCVD) method. Subsequently, the nitridation of the films was carried out by a microwave-excited plasma using a gas mixture of  $\text{N}_2$  and Ar, and followed by  $\text{N}_2$  annealing at  $1050^{\circ}\text{C}$ . The chemical composition and bonding features of the samples so prepared were characterized by measuring core line spectra such as Hf4f, Si2p, N1s and O1s spectra excited by monochromatized  $\text{AlK}\alpha$  (1486.6eV) radiation. The energy distribution of filled defect states in the dielectric layer was evaluated by total photoelectron yield spectroscopy (PYS) in the photon energy range of 4-6eV. For the depth profiling of the chemical structures and the defect state densities in the dielectrics, XPS and PYS measurements were conducted repeatedly at each thinning step of the dielectric layer in a dilute HF solution. The experimental details for PYS measurements were described elsewhere (8).

## Results and Discussion

The changes in chemical bonding features in  $\text{HfSiO}_x\text{N}_y$  with  $\text{N}_2$ -annealing at  $1050^{\circ}\text{C}$  were first evaluated by analyzing core line spectra taken before oxide thinning. For simplicity, each of measured Si2p and Hf4f spectra was deconvoluted into two components in consideration with spin-orbit splitting of each core line. For the samples

before N<sub>2</sub> annealing, chemically-shifted Si2p(3/2) signals in the lower binding energy side become significant with increasing average nitrogen content as shown in Fig. 1(a). This spectral change is simply explained as an increase in Si-N bonding units and a decrease in Si-O bonding units as also confirmed from changes in N1s and O1s spectra. The N<sub>2</sub>-annealing at 1050°C causes a further increase in Si-N bonds as clearly seen in annealing the sample with an average N content of 20.5at% (Fig. 1(b)) but a decrease in the average N content. A distinct change in chemical bonding features of Hf ions was

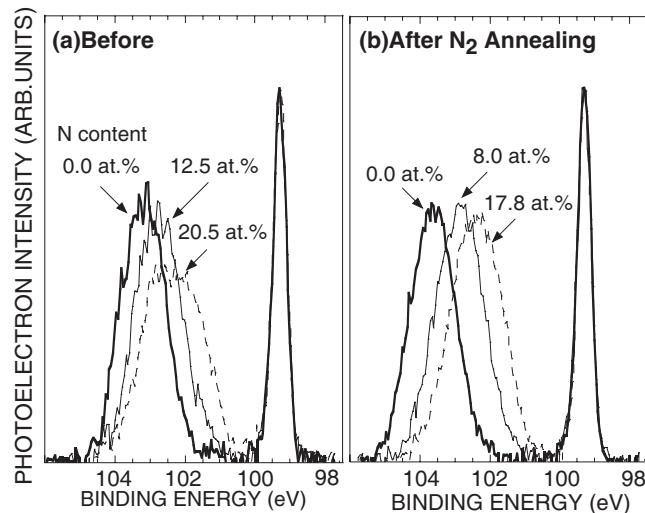


Fig. 1 Si2p(3/2) spectra for ~5nm-thick HfSiO<sub>x</sub>N<sub>y</sub> (Hf/(Hf+Si)~43%)/Si(100) (a) before an (b) after N<sub>2</sub> annealing at 1050°C. The binding energy was calibrated by the Si2p(3/2) peak at 99.3eV for the Si(100) substrate and the photoelectron intensity was normalized by the peak intensity of Si2p(3/2) signals from the Si(100) substrate. The take-off angle of photoelectrons was set at 90°. By the N<sub>2</sub> annealing, the average nitrogen contents of 12.5 and 20.5 at.% were decreased to 8.0 and 17.8at.%, respectively.

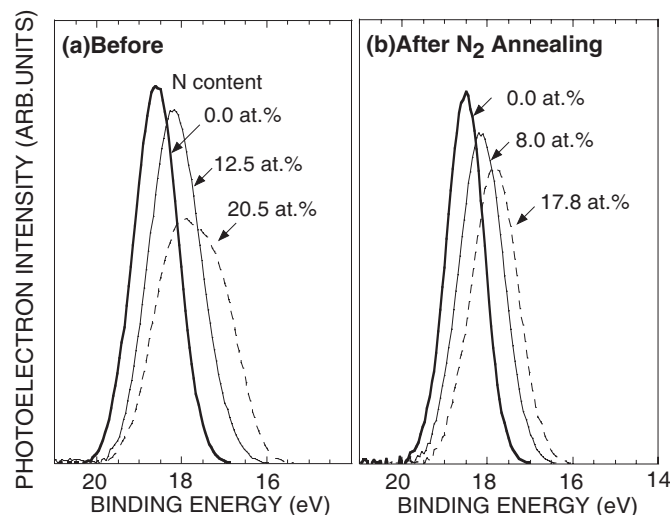


Fig. 2 Hf4f(7/2) spectra for ~5nm-thick HfSiO<sub>x</sub>N<sub>y</sub> (Hf/(Hf+Si)~43%)/Si(100) (a) before an (b) after N<sub>2</sub> annealing at 1050°C. The binding energy and the relative intensity scales were treated the same as Fig. 1. The take-off angle of photoelectrons was set at 90°.

also observed as represented in Fig. 2. For the samples before the N<sub>2</sub> annealing, a significant broadening of Hf4f(7/2) signals toward the lower binding energy side with increasing N content indicates an increase in highly-nitrided Hf ions in the dielectric (Fig. 2(a)). And the spectral change attributable to the thermal dissociation of such highly-nitrided components is clearly observed (Fig. 2(b)). Thus, the released N atoms from Hf-N<sub>x</sub> bonds are responsible for an increase in Si-N bonding units.

The chemical bonding features of Hf ions were characterized from the spectral analysis of Hf4f spectra as demonstrated in Fig. 3. For the non-annealed sample with an average N content of 20.5at.%, the observed spectrum consists of four components with the same spectral width as the spectrum of the sample without nitridation (Fig. 3(a)). In the spectral deconvolution, the energy shifts for the components were set at 0, 0.45, 0.95 and 1.5eV towards the lower binding energy side from the peak of the sample without nitridation. The energy shift toward the lower binding energy side is attributable to an increase in the number of coordinate N atoms around one Hf ion. Considering the ratio of N content to O content, quite a large percentage of Hf ions have three N atoms each, which implies the localization of N incorporation. In the spectrum taken after N<sub>2</sub> annealing, one component in the lowest binding energy side disappears and other three components remain (Fig. 3 (b)). As a result of thermal dissociation of Hf-N<sub>3</sub> bonding units, the Hf-N<sub>2</sub> bonding units increase remarkably. Also, since no significant increase in the Hf-N bonding units is observable, N atoms released from Hf-N<sub>3</sub> bonding units can promote substitution reaction for O atoms in Si-O-Si bonding units in the dielectric and in the interfacial silicon oxide layer as discussed later. As shown in Fig. 4, even in the annealed sample with an average N content as low as ~4.5at.%, the concentration of the

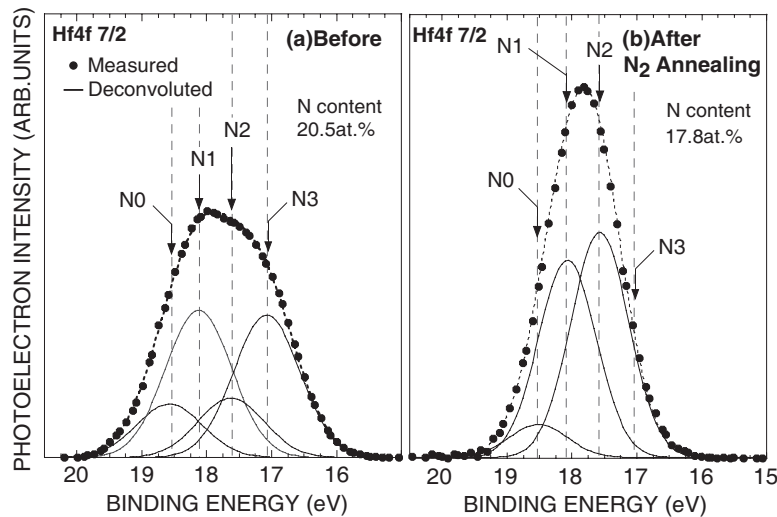


Fig. 3 Hf4f(7/2) spectra and their components for a couple of samples before and after annealing shown in Fig. 2. The N0 component is identical to the spectrum for the sample without nitrogen atom. The components denoted by N1, N2, and N3 are attributed to Hf ions coordinated with one, two and three nitrogen atoms, respectively. In the spectral deconvolution, the spectral width of each component kept constant at 1.20eV for the sample before annealing and at 1.07eV for the sample after annealing. With an increase in the number of coordinate nitrogen atoms, the chemical shift toward the lower binding energy side is increased by 0.45eV for one nitrogen atom, 0.95eV for two nitrogen atoms and 1.50eV for three nitrogen atoms.

Hf ions having one N atom as a coordinate is almost equal to that of the Hf ions coordinated all with O atoms. Also the Hf-N<sub>3</sub> component is observable even for 8 at.% in average N content and increases in directly proportional to the average N content. There seems to be a situation for N atoms to coordinate preferentially to Hf ions rather than Si atoms, presumably because O vacancies tend to be generated around Hf ions.

As the next step, to get some information on the depth profile of the chemical composition and bonding features without oxide thinning, the core line spectra were measured at different take-off angles of photoelectrons. Figure 5 shows the results obtained for the annealed sample with an average N content of 8.0at.%. All the spectrums were normalized with chemically-shifted Si2p<sup>4+</sup>(3/2) peak originating from the dielectric. With decreasing photoelectron take-off angle, the Si2p<sup>0+</sup>(3/2) signals peaked at 99.3eV originating from the Si(100) substrate are reduced significantly because of the attenuation of photoexcited electrons passing through the dielectric layer. Considering

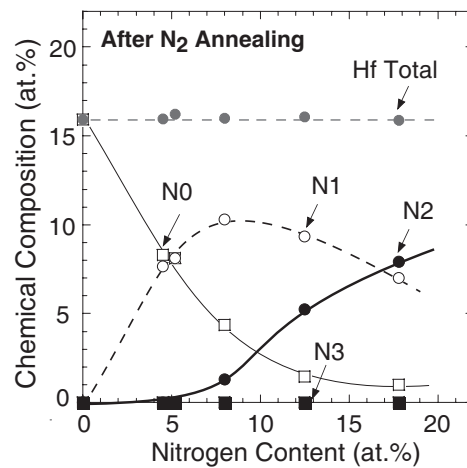


Fig. 4 Atomic percentages of Hf-N<sub>x</sub> (x=0~3) components summarized as a function of the average N content. The notification of each component is the same as Fig. 1.

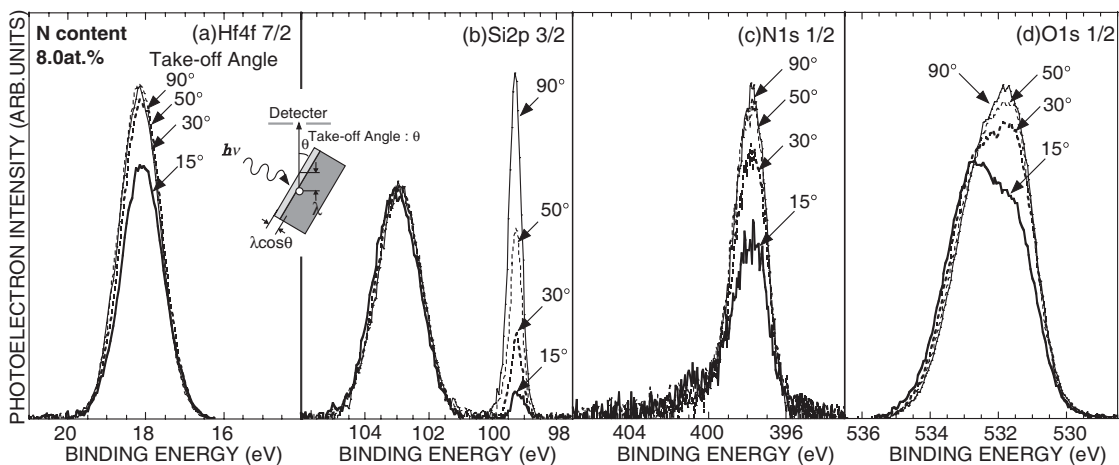


Fig. 5 (a) Hf4f(7/2), (b) Si2p(3/2), (c) N1s and (d) O1s spectra of an annealed sample with an average N content of 8.0at.%, which were taken at photoelectron take-off angles of 15, 30, 50 and 90°.

that the lower binding energy component of O1s signals is attributed to Hf-O bonding units, observed decreases in Hf4f(7/2), N1s and O1s signals implies the formation of Si-enriched oxide region at the sample surface.

For in-depth profiling on the chemical structures of annealed samples, the XPS measurements were carried out at each step of wet-chemically etching of the HfSiO<sub>x</sub>N<sub>y</sub> layer. Figure 6 shows the results obtained for the annealed sample with an average N content of 8.0at.% as well. No change in surface microroughness by the oxide thinning was confirmed by AFM observations. With progressive thinning of HfSiO<sub>x</sub>N<sub>y</sub>, the chemically-shifted Si2p signals and O1s signals in the higher binding energy side become dominant as a result of a decrease in main component, indicating the presence of the interfacial silicon oxide layer. The N incorporation into the interfacial layer was confirmed by a dilute HF etching for 66 sec, in which no Hf4f signals were detectable but N1s signals were still observable. In the depth profile of chemical composition

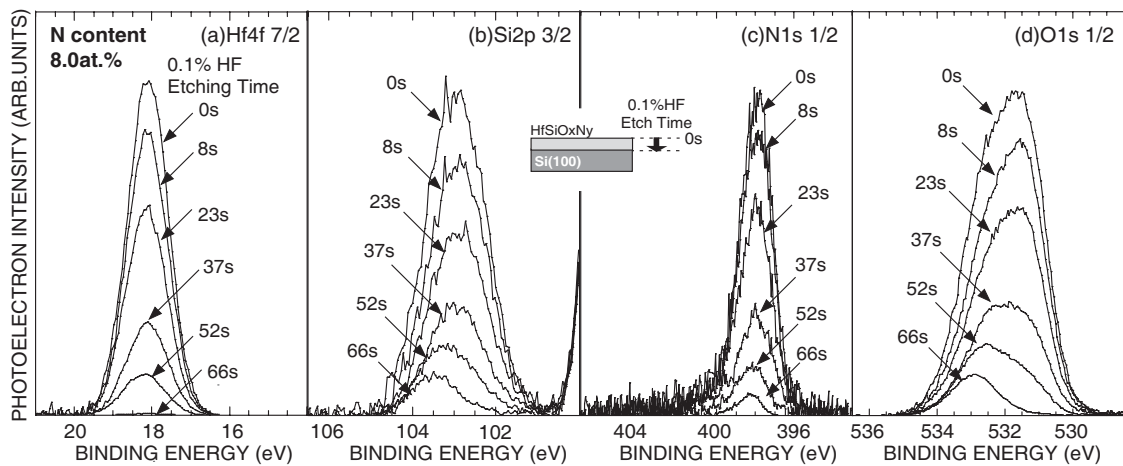


Fig. 6 (a) Hf4f(7/2), (b) Si2p(3/2), (c) N1s and (d) O1s spectra of the annealed sample shown in Fig. 5 with progressive oxide thinning by a dilute HF etching.

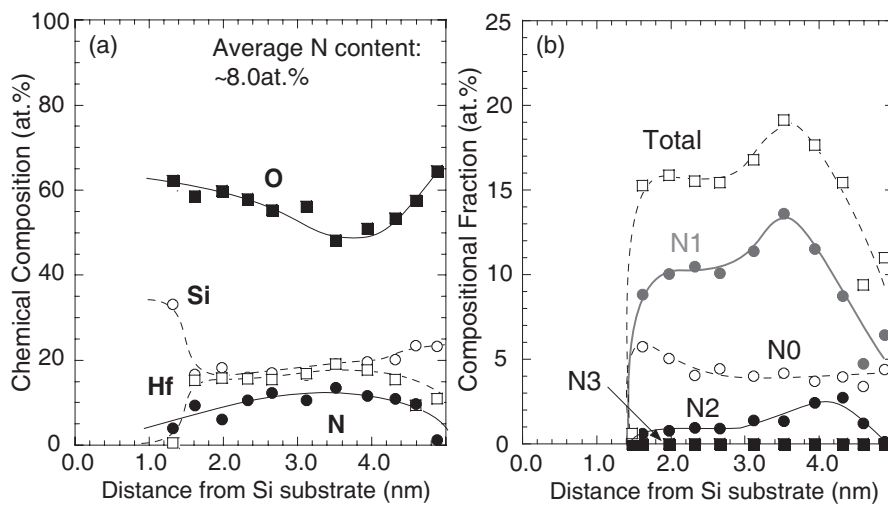


Fig. 7 Depth profiles of (a) chemical compositions and (b) components in Hf-N<sub>x</sub>(x=0~3) bonding units measured for the sample shown in Figs. 5 and 6, which were determined from the changes in core line signals at each step of oxide thinning.

determined from the change in the intensity at each thinning step as shown in Fig.7, there is a region with an oxygen content as low as  $\sim 50$  at.% around  $\sim 1.2$ nm from the surface and Hf-N and Hf-N<sub>2</sub> bonding units distribute with peaks around  $\sim 1.5$ nm and  $\sim 0.8$ nm from the top surface, respectively. The inhomogenous profile of the chemical compositions is more pronounced for the sample with an average N content of  $\sim 17.8$ at.% as represented in Fig. 8. Obviously, the O content becomes its minimum around  $\sim 1.2$ nm from the surface while the N content becomes its maximum around  $\sim 1.5$ nm from the top surface and Hf-N<sub>2</sub> bonding units becomes dominant within 2nm from the surface. The result suggests that the surface re-oxidation occur concurrently with the diffusion of N atoms generated by thermal decomposition of the Hf-N<sub>x</sub> units during the N<sub>2</sub>-annealing.

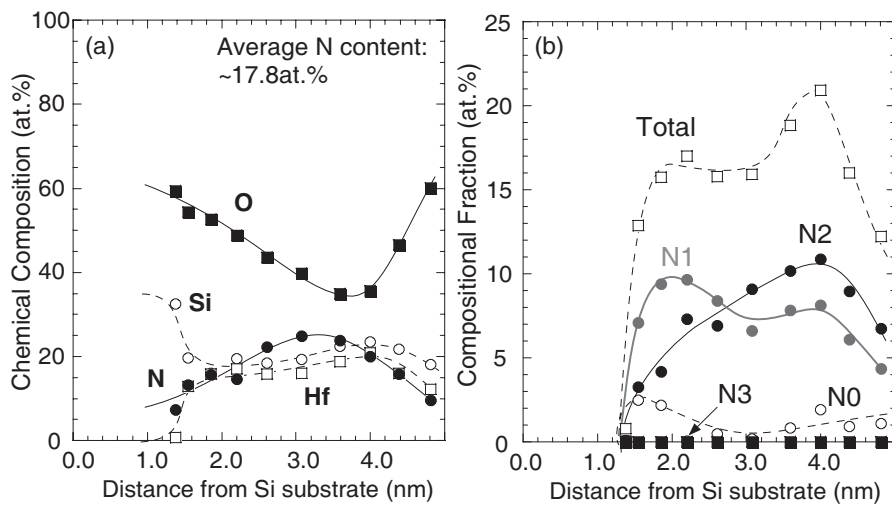


Fig. 8 Depth profiles of (a) chemical compositions and (b) components in Hf-N<sub>x</sub>(x=0~3) bonding units measured for the annealed sample with an average N content as high as 17.8at.%, which were determined from the changes in core line signals at each step of oxide thinning.

The energy distribution of electronic defect states in ultrathin dielectrics and at dielectric/Si(100) interfaces can be evaluated without gate fabrication by total photoelectron yield spectroscopy (PYS) being unconstrained by the leakage current (8). As shown in Fig. 9, the photoelectron yields from the samples after N<sub>2</sub>-annealing at 1050°C measured as a function of photon energy in the range from 4.0 to 6.0eV. The valence electrons in the HfSiO<sub>x</sub>N<sub>y</sub> layers can not be emitted out by irradiation of photons in this energy range (9, 10). Therefore, the photoelectron yields in the energy region below 5.15eV, corresponding to shallower than the Si valence band (VB) edge, are attributable to the emission from filled defect states distributed in the dielectric and at the interface. The photoelectron yield due to defect states near the Si VB edge is increased gradually with the average N content up to 8.0at.% while it tends to be saturated in the range of 8.0-12.5%. A further increase in the N content up to 17.8at.% causes a dramatic increase in the photoelectron yield. For the sample without N content, the crystallization accompanied with phase separation, which was confirmed by TEM observations, may involve in the generation of defects showing a large yield in the energy region deeper than the Si VB edge.

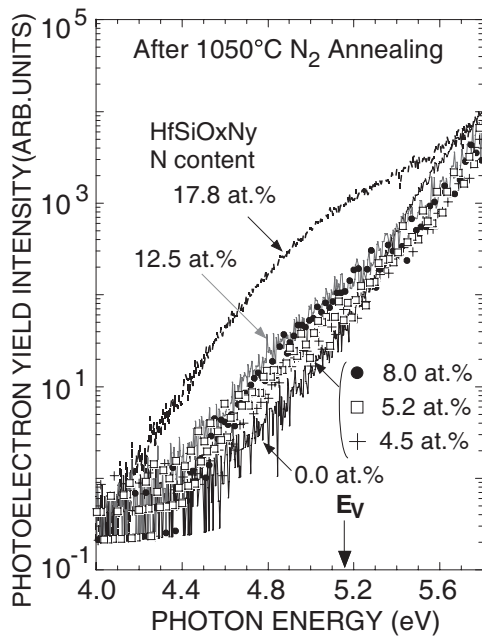


Fig. 9 Total photoelectron yield spectra for the annealed samples with different average N contents.  $E_v$  denotes the Si valence band top measured from the vacuum level.

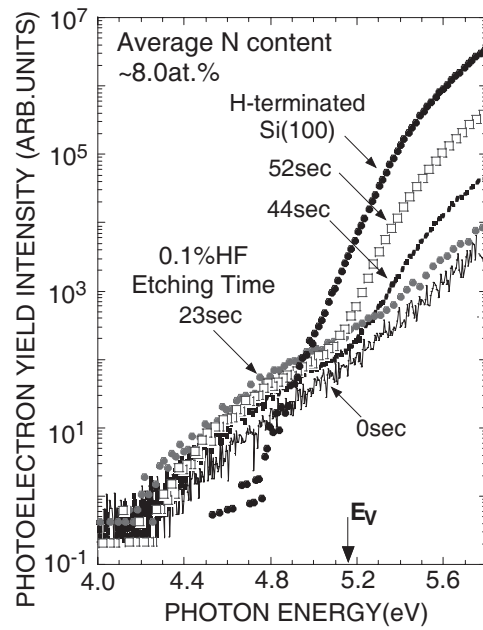


Fig. 10 Total photoelectron yield spectra measured with progressive oxide thinning of the annealed sample with an average N content of 8.0 at.%. In the oxide thinning, a 0.1% HF solution was used. The yield spectrum for H-terminated Si(100) prepared by a dilute HF etching is also shown as a reference.

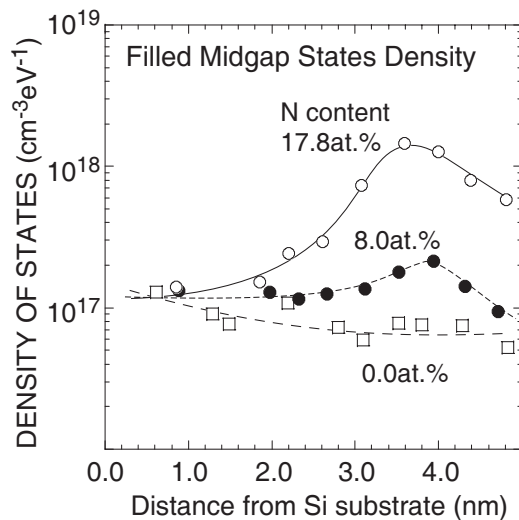


Fig. 11 Depth profiles of filled defect states at an energy position corresponding to Si midgap for the annealed samples with average N content of 0, 8.0 and 17.8 at.%, which were determined from the changes in PYS spectra with progressive oxide thinning as typically seen in Fig. 10, by using the same method as described in Ref. 8.

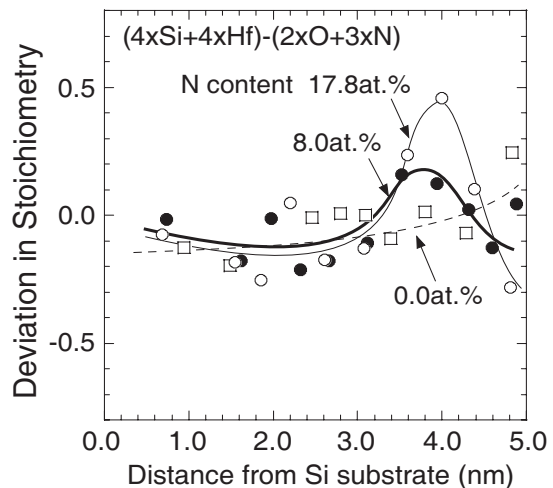


Fig. 12 Deviation in stoichiometry estimated from the difference between anion and cation valences for the annealed samples shown in Fig. 11. In the calculation, it is assumed that Si and Hf atoms are tetravalent, and O and N atoms are divalent and trivalent, respectively.



To get a clear insight into the increase in defects with N incorporation, the PYS measurements were performed with progressive oxide thinning as shown in Fig. 10. Obviously, the photoelectron yield above 5.15eV, which is due to valence electrons from the Si substrate, became significant with progressive oxide thinning. As for the photoelectron yield due to the defects, it increased with the etching time up to 23sec and then decreased with further progressive thinning. Figure 11 shows the depth profile of the defect states derived from the change in the yield by using the same procedure as described in Ref. 8. For the sample with no N content, the defect states of  $\sim 7 \times 10^{16} \text{ cm}^{-3}/\text{eV}$  distribute homogeneously. In contrast, with increasing N content, the defect state density in the near-surface region, where oxygen deficiency and Hf-N<sub>2</sub> bonding units become significant as represented in Figs. 7 and 8, is markedly increased up to the level as high as  $\sim 1 \times 10^{18} \text{ cm}^{-3}/\text{eV}$  for the sample with 17.8at.% in average N content. Considering the balance in valency between anions and cations, a significant deviation from binding stoichiometry occurs in near-surface region as shown in Fig. 12, which is likely to closely correlate with the defect generation.

### Summary

For  $\sim 5\text{nm}$ -thick HfSiO<sub>x</sub>N<sub>y</sub> (Hf/(Hf+Si)=43%) on Si (100), chemical bonding features and electronic states were evaluated from XPS and PYS measurements. The analysis of core line spectra show that Hf-N<sub>x</sub> ( $x \geq 2$ ) bonding units are generated by plasma nitridation and markedly reduced by 1050°C annealing to form Si-N bonding units together with the oxynitridation of Si(100) substrate. For the annealed sample with average N contents of 8.0 and 17.8at.%, an oxygen deficient region is formed near the surface. The PYS analysis shows that, for the annealed samples, the defect state density is increased with the N content and becomes its maximum in the oxygen deficient near-surface region. It is suggested that the imbalance in chemical coordination between anions and cations is responsible for the defect generation.

### Acknowledgments

The authors wish to thank Dr. H. Murakami and Assoc. Prof. S. Higashi for their assistance, and the members of the research project “High-k Net” for their fruitful comments and discussion.

### References

1. For example: “High Dielectric Constant Materials”, Eds H. R. Huff and D. C. Gilmer (2004, Springer).
2. G. D. Wilk, R. M. Wallace and J. M. Anthony: J. Appl. Phys. **89**, 5243 (2001).
3. G. D. Wilk, R. M. Wallace and J. M. Anthony: J. Appl. Phys. **87**, 484 (2000).
4. M. Yamaoka, A. Ohta and S. Miyazaki: Ext. Abstr. Int. Conf. Solid State Devices & Material, p.810, Tokyo (2003).
5. M. R. Visokay, J. J. Chambers, C. H. Chen, A. L. P. Rotondaro, A. Shanware and L. Colombo: Appl. Phys. Lett. **80**, 3188 (2002).

6. M. Koyama, A. Kaneko, T. Ino, M. Koike, Y. Kamata, R. Iijima, Y. Kamimuta, A. Takashima, M. Suzuki, C. Hongo, S. Inumiya, M. Takayanagi and A. Nishiyama : IEDM Tech Dig., p.847, San Francisco (2002).
7. H.C.-H. Wang, C.-W. Tsai, S. Chen, C.-T. Chan, H.-J. Lin, Y. Jin, Y. Jin, H.-J. Tao, S.-C. Chen, C. H. Diaz, T. Ong, A. S. Oates, M.-S. Liang and M.-H. Chi, Deg. Tech. Papers of Symp. on VLSI Technol., p.17, Kyoto (2005).
8. S. Miyazaki, T. Maruyama, A. Kohno and M. Hirose, Microelec. Eng., **48**, 63 (1999).
9. A. Ohta, H. Nakagawa, H. Murakami, S. Higashi, S. Miyazaki, S. Imumiya and Y. Nara, Trans. of Mat. Res. Soc. of Jpn., **31**, 125 (2006).
10. S. Miyazaki, A. Ohta, Y. Pei, S. Inumiya and Y. Nara, *Proc. of E-MRS IUMRS ICEM 2006 Spring Meeting (Nice, 2006) to be published.*